Global NEST Journal, Vol 24, No 2, pp 276-285

Adsorption isotherm and kinetic studies for the decolorization of sunset yellow FCF dye using economically feasible low-cost adsorbent

Nafisa Begam M.N.[1*], Muthukumaran K.[2], Thamarai P.[3], and Joshua J.P.[4]
[1]Department of Industrial Biotechnology, Government College of Technology, Coimbatore-641013, India
[2]Department of Chemistry, Government College of Technology, Coimbatore-641013, India
[3]Department of Environmental Engineering, Government College of Technology, Coimbatore-641013, India
[4]Department of Physics, The New College (Autonomous), Chennai – 600014, India
Received: 27/01/2022, Accepted: 19/03/2022, Available online: 28/03/2022
*to whom all correspondence should be addressed: e-mail: nafisa.mn.ibt@gct.ac.in
https://doi.org/10.30955/gnj.004266

Graphical abstract

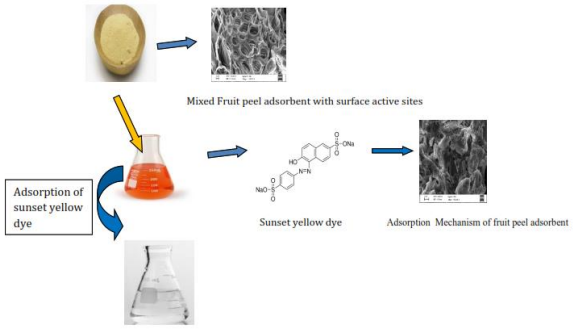

Abstract

The present communication attempts to explore the adsorption potential of Mixed Fruit Peel Waste (MFPW) to remove Sunset Yellow FCF dye from an aqueous solution. The MFPW is a low-cost adsorbent prepared from the peels orange, watermelon and banana. The characterization of MFPW was made through FTIR, SEM and BET studies. The FTIR studies revealed the presence of functional groups such as nitro, carboxyl, ester, ether, phenol and alkyne that are solely responsible for adsorption. The surface morphology exposed the clear and well-developed pores of MFPW. Batch adsorption studies resulted in a maximum adsorption capacity (q_{max}) of 200 mg/g at optimum pH 3.0, contact time of 100 minutes, and adsorbent dose of 2.0 g/L with an initial dye concentration of 40 ppm. Sunset Yellow FCF dye removal was discovered to be spontaneous and endothermic in nature, with the Langmuir isotherm and pseudo-second-order-kinetics providing the best fit. In summary, mixed fruit peel waste adsorbent can be used as a low-cost, environmentally friendly and sustainable adsorbent to decolorize sunset yellow FCF dye.

Keywords: Adsorption, sunset yellow, mixed fruit peel waste adsorbent.

1. Introduction

Dye effluents are released during the dyeing process in the textile, food, printing, leather, plastic, and cosmetic industries [Hejun Gao *et al*., 2013; Yu Zhiyong *et al*., 2013]. These dye effluents have an impact on groundwater quality by altering parameters like Biological Oxygen Demand (BOD), Chemical Oxygen Demand (COD), Total Organic Solids (TOS), Total Dissolved Solids (TDS), and Total Suspended Solids (TSS) [Garba Z.N *et al*., 2019; Xiaoduo Liu *et al*., 2019]. It is also known that dye effluents cause eutrophication (the blocking of sunlight), depleting nutrients in the water and endangering aquatic life. Nonetheless, consuming such polluted water has a significant impact on terrestrial life, resulting in serious health issues such as asthma, cancer, skin and throat irritation, and so on. As a result, proper treatment of dye effluents from industries has become critical [Rangabhashiyam *et al*., 2017].

There are currently several treatment options available, including filtration, precipitation, membrane separation, ion exchange, coagulation, flocculation, and adsorption, with the adsorption method being versatile, cost-effective and ease of operation [Jayalakshmi and Jeyanthi, 2021; Zhifeng Jiang *et al*., 2014; Yonggang Liu *et al*., 2010]. Researchers have developed various adsorbents to remove dye effluents from the environment, such as activated carbon, sawdust, bagasse fly ash, guava seeds, nanocomposites, lignocellulosic biomass, and agricultural byproducts such as fruit peels, wheat, and rice bran. But many adsorbents fail to meet the minimum requirements for wastewater recycling, such as high selectivity and good adsorption capacity for wastewater recycling [Garg *et al*., 2003; Mall, Indra *et al*., 2006]. However, due to its high adsorption capacity, various fruit waste has been highlighted as an adsorbent in previous studies [Husseien *et al*., 2007; Ranjithkumar *et al*., 2017].

Among other adsorbents, fruit waste adsorbents are cost-effective, sustainable, biocompatible, easy to scale up and environmentally friendly, making them a promising

candidate for wastewater treatment. Moreover, water material utilization can bridge the gap between the water-energy-food circular economies [Hossain *et al*., 2020; Solangi *et al*., 2021]. Previous research has shown that noncarbonized guava seeds effectively adsorb selective azo and anthraquinone dyes. Similarly, Methylene Blue, Eriochrome Black T., and Alizarin S dyes can be removed using dried prickly pear cactus cladodes adsorbent [Barka *et al*., 2009; Machrouhi *et al*., 2017]. The peels of *Punica granatum L*. were found to adsorb 98.07 %of Pb (II) ions and 94.76 % of Acid Blue 40 from industrial wastewaters. Rhodamine B and Methylene Blue were removed using digested fruit waste [Hussain *et al*., 2016; Bhatnagar, Amit *et al*., 2009].

The adsorbent behavior of mixed fruit biomass for removing dyes in the literature was insignificant so far. However, the effectiveness of activated carbon derived from fruit waste as an adsorbent was reported in many studies [Wong *et al*., 2018; Sahu *et al*., 2020; Ramalingam *et al*., 2020]. Moreover, the studies reported that biomass could be a potential substitute for activated carbon, reducing operational costs [Rebitanim *et al*., 2012]. Therefore, an attempt was made to prepare mixed fruit peel waste biomass cost-effectively and efficiently, without chemical or thermal activation in this study. Furthermore, its corresponding adsorptive behavior for dye removal was studied. Moreover, the reported adsorption capacity of mixed fruit peel waste is higher when compared to other fruit waste as well as activated carbons [Lim *et al*., 2020; Nguyen *et al*., 2020].

This study investigates the utilization of mixed fruit peel (orange, watermelon, and banana waste peels) as adsorbents for removing sunset yellow FCF dye. First, the mixed fruit peel waste adsorbent's morphology and chemical properties are well-characterized using FTIR spectroscopy and SEM analysis. Then, batch adsorption studies were conducted to assess its adsorptive behavior for sunset yellow FCF dye from an aqueous solution. And the biosorption efficiency of mixed fruit peel waste adsorbent is evaluated by optimizing the effects of pH, contact time, adsorbent dosage, initial dye concentrations and temperature. Finally, the results from the batch adsorption studies were validated using isotherm, kinetics, and thermodynamic studies.

2. Experimental set up

2.1. Methods and materials

This study only used analytical-grade chemical reagents. The Sunset Yellow FCF (SY FCF) textile dye was purchased from Sigma-Aldrich and used without further purification. Deionized water was used to prepare the Sunset yellow dye stock solution, then used to prepare various concentrations of solutions. The pH was adjusted with a solution of HCl and NaOH. Each experiment necessitated the use of brand-new dilutions. Orange, watermelon, and banana peels were purchased from a nearby juice shop and washed in deionized water. They were finely chopped into small pieces to make crushing easier. The peels were kept in a hot air oven at 70°C for 48 hours. After drying, the pieces were ground into a fine powder in a mixer grinder and sieved through a 150 µm mesh sieve to obtain uniformly sized particles. Finally, the powdered mixed fruit peel waste was stored in an airtight container for future use. [Bhatnagar *et al*., 2021; Khaskheli *et al*., 2021].

2.2. Characterization of prepared adsorbent

FTIR spectra were used to investigate the chemical functional groups of the adsorbent, and the adsorbent was loaded as KBr discs and recorded in a Fourier Transform Infrared Spectrophotometer (PerkinElmer Spectrum Two). A surface area analyzer was used to investigate mixed fruit peel waste's pore size, surface area, and pore volume (BELSORP-Mini II). The adsorbent's surface morphology was investigated using a scanning electron microscope (ZEISS). A UV–Visible spectrophotometer (Systronics) was used to measure the absorption of sunset yellow dye (λmax=482 nm). The pH of the aqueous solutions was determined using a Labman model pH metre with a glass electrode [Ahmad *et al*., 2021; Almeida-Naranjo *et al*., 2021].

2.3. MFPW point of zero charge determination

The salt addition method was used to determine the adsorbent's net neutral charge. Using 0.1M HCl/NaOH, the initial pH of the 0.1M potassium nitrate solutions was set in the range of 2.0 – 10.0. 0.1 g of MFPW adsorbent was added and agitated at 120 rpm for 24 hours. The final pH of the solution was recorded. The zero-point charge of the adsorbent was determined by drawing a graph between ΔpH and initial pH [Solangi *et al*., 2021].

2.4. Biosorption experiments

Batch adsorption studies using mixed fruit peel waste powder were carried out to optimize process parameters such as pH, contact time, adsorbent dosage, initial dye concentration and temperature. The pH was adjusted with HCl and NaOH, and residual concentrations were determined using a standard graph in a UV-Visible spectrophotometer. The experiments were carried out with a stock dye solution containing 20mg/L of SY-FCF, and parameters such as contact time (5.0 – 200 minutes), adsorbent dosages (0.5-2.0g), and pH were varied (3-10).

2.5. Isotherm and kinetic studies

Two grams of adsorbent were used in a series of conical flasks with initial dye concentrations (10-50mg/L) at pH 3.0 for adsorption equilibrium studies. In a rotary orbital shaker (Scigenics), the flasks were incubated for 60 minutes at 120 rpm. The concentration of the treated SY FCF dye solution was determined at 482nm using a UV-Visible spectrophotometer after the adsorbent was removed from the supernatant. The equilibrium adsorption rate (q_e) was given in equation 1, and the percentage of dye removal was calculated from equation 2:

$$q_e = \frac{(C_0 - C_e) * V}{m} \quad (1)$$

where q_e (mg/g) is defined as the quantity of dye adsorbed per unit mass of adsorbent, C_o & C_e are initial and final dye

concentration (mg/L), V is the volume of the SY FCF dye solution and m is the mass of the adsorbent, respectively [Gupta *et al*., 2021]. Meanwhile, Removal efficiency is calculated as follows.

$$\%Removal = \frac{(C_0 - C_e)}{C_0} * 100 \quad (2)$$

3. Results and discussion

3.1. Characterisation of adsorbent

3.1.1. FTIR Studies

FTIR peak of the MFPW adsorbent before and after adsorption (Figure 1) was evaluated to identify the functional groups responsible for SY FCF adsorption.

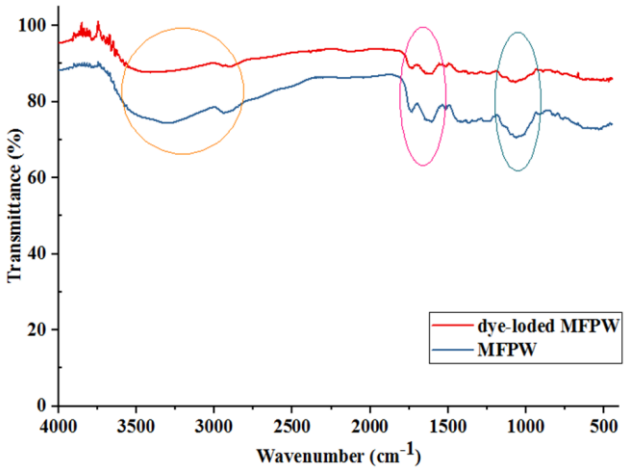

Figure 1. FTIR spectra of MFPW and dye-loaded MFPW.

Table 1 shows the FTIR spectrum of MFPW and dye-loaded MFPW. The adsorption capacity may be affected by the chemical reactivity of the surface functional group. The fruit peel comprises cellulose and pectin, and signals corresponding to O-H, C-O, C-H, and C-C bonds were found. After adsorption, the peaks at 2937.82cm^{-1} and 1300-1600cm^{-1} vanish, indicating that the C-C stretching of the alkyne group and C-H bending in a carboxylic acid functional group is responsible for SY FCF adsorption onto MFPW [Idris *et al*., 2011; Sun*et al*., 2010]. Furthermore, the rest of the peaks in MFPW have shifted to lower intensity after the SYFCF adsorption onto MFPW. Adsorption is attributed to functional groups such as nitro, carboxyl, ester, ether, phenol, and alkyne groups.

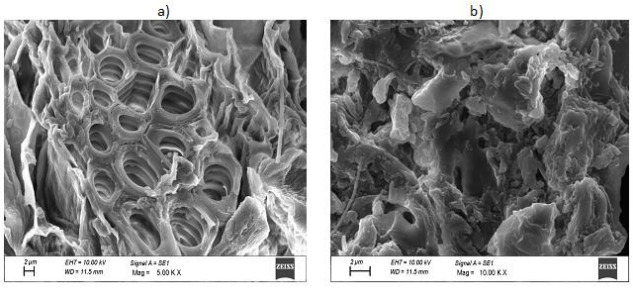

Figure 2. SEM micrograph of MFPW and dye-loaded MFPW.

3.1.2. Surface morphology

Before and after SY FCF adsorption, the surface morphology of the mixed fruit peel waste was observed at 2 µm magnification of the adsorbent. Figure 2(a) showed that the surface morphology is clear and has well-developed pores. The pore development could be due to the activation of pores during thermal expansion. These pores allow dye molecules to come and sit on its. Therefore, the MFPW's adsorption capacity may be influenced by the pore size and pore volume of adsorption sites to accumulate a more significant number of dye molecules. [Auta *et al*., 2011; Aksu *et al*., 2010; Shoukat *et al*., 2017]. Figure 2(b) shows that the surface of MFPW was covered with dye molcules.

Table 1. Different functional groups identified by FTIR spectra before and after adsorption

Functional group	Before adsorption Wavenumber(cm^{-1})	After adsorption Wavenumber(cm^{-1})
O-H stretching of hydroxyl group	3787.72	3637.18
C-C stretching of alkyne group	2937.82	-
C-O stretching vibrations in quinine structure	1610.12	1605.59
C-O group stretching in ester, ether or phenol groups	1243.79	1237.17
C-N stretching of aliphatic primary amines	1065.35	1069.47
CH_3 or CH_2 groups bending vibration in carboxylic acid	1369.76-1578.51	-
C-H bending in functional group	535.29	470.78-672.44

The MFPW was investigated using N_2 adsorption/desorption isotherm studies to study the porosity and surface area. And the corresponding BET plot was depicted in Figure 3. The MFPW's surface area, total pore volume, and mean pore diameter before and after adsorption were found to be 2.5 m^2/g, 0.0045cm^3/g, 7.25nm, and 0.2 m^2/g, 0.00024cm^3/g, 4.06nm, respectively. It is understood that raw adsorbents have a larger surface area and pore volume, indicating that the adsorption cavities are receptive to dye molecules. Furthermore, the values in the recovered adsorbents are reduced following the adsorption studies. This corresponds to the BET surface area of *P. granatum L*. peels [16]. The surface area and pore diameter of the adsorbent are highly dependent on the adsorption sites, which are highly advantageous for effective dye adsorption. Since the mixture of fruit peel waste has a different surface area, the dye molecules can easily attach to the adsorption site, which can be predicted using the sample's pore volume [Idris *et al*., 2011].

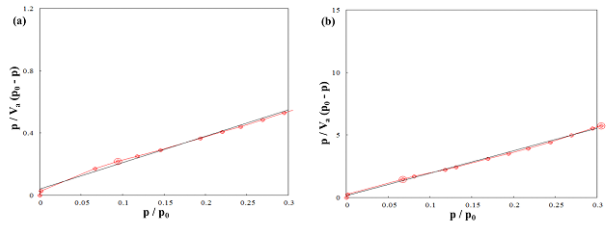

Figure 3. BET studies for MFPW and dye-loaded MFPW.

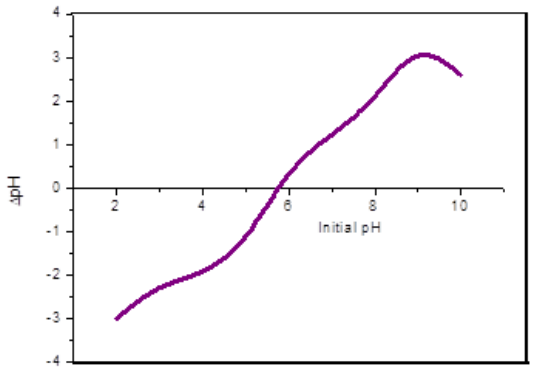

Figure 4. P_{ZPC} of the biosorbent.

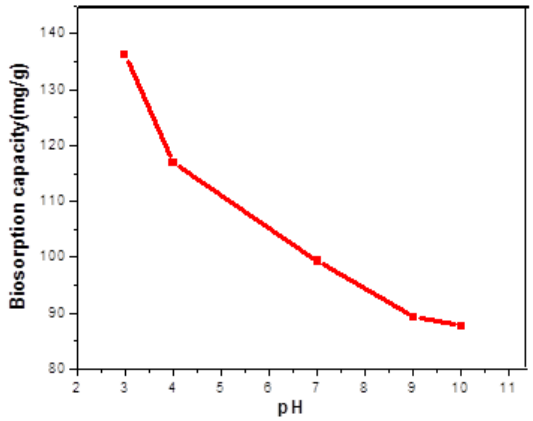

Figure 5. Effect of pH for the adsorption of sunset yellow dye using MFPW adsorbent.

3.2. Point of Zero charge and effect of pH

Figure 5 shows the effect of pH on SY FCF adsorption using mixed fruit peel waste. And the adsorption was conducted with initial concentration 50mg/L, shaking speed 120rpm, adsorbent dose 2.0 g/100mL, pH 3-10, contact time 120 mins, temperature 30°C.

MFPW biosorbent was discovered to have a P_{ZPC} of nearly 5.9, as shown in Figure 4. As a result, pH levels above and below 5.9 may be optimal for dye adsorption. Because the proteins and amino acids in the mixed fruit peel waste are easily ionised in dye solutions, they affect the charged surface of the adsorbent [Aksu *et al*., 2010; Shoukat *et al*., 2017]. Pzpc of the biosorbent is more positively charged at acidic pH, making it more attractive for the adsorption of sunset yellow, which belongs to the anionic dyes. Because hydroxyl ions are present, pH above 5.9 is negatively charged, allowing anions to be repelled under these conditions. The biosorption of an anionic dye sunset yellow was found to be optimal at pH 3.0, indicating that positively charged ions on the surface of an adsorbent are favourable for anion attraction, as demonstrated by the results of this study. The adsorption capacity of sunset yellow dye was measured at 136.16mg/g at pH 3.0 and gradually decreased to 87.7mg/g at pH 10.

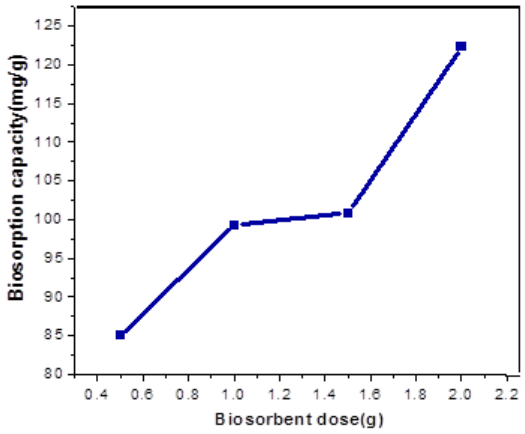

Figure 6. Effect of biosorbent dose for the adsorption of sunset yellow dye using MFPW adsorbent.

3.3. Effect of biosorbent loading:

Figure 6 shows the effect of MFPW dose on SY FCF removal. The experiments were conducted under the conditions of pH 3.0, initial dye concentration 50mg/L, shaking speed 120rpm and adsorbent dose 0.5-2g/100ml) for 120 minutes at 30°C.

The biosorbent dose is regarded as a critical parameter in the process for ensuring the viability of the adsorption process. The MFPW adsorbent doses ranged from 0.5 to 2.0 g/100mL. Initially the experiment was carried out with a dye concentration of 50 mg/L at pH 3.0. Sunset yellow dye adsorption required 2.0g of mixed fruit peel waste due to the large number of surface adsorption sites [Shoukat *et al*., 2017]. Therefore, the percentage removal of dye was slightly increased between 0.5 and 1.5 g/100 mL of dye solution because there were fewer adsorption sites. Still, it reached its maximum at 1.5-2.0 g/100 mL of dye solution due to the large number of active sites on its surface, as shown in Figure 6. As a result, biosorbent dose of up to 2.0 g/100mL is recommended for future experiments.

3.4. Effect of initial dye concentration and biosorption isotherms:

Langmuir, Freudlich, Temkin, Dubinin-Radushkevich and Harkins -Jura adsorption isotherm model to study the adsorption of Sunset Yellow FCF dye onto mixed fruit peel waste adsorbent.

Langmuir isotherm model is represented by the equation 3

$$\frac{C_e}{q_e} = \frac{1}{bq_{max}} + \frac{C_e}{q_{max}} \qquad (3)$$

Where C_e (equilibrium concentration), q_e (adsorption capacity), q_m (Langmuir maximum adsorption capacity). The Langmuir constants q_m and K_L are calculated from the slope and intercept of linear plot between C_e/q_e *vs* C_e.

The linear form of Freundlich isotherm model is given by equation 4

$$\log q_e = \log K_f + \frac{1}{n}\log C_e \quad (4)$$

The plot between Log q_e versus Log C_e provides the slope 1/n and the intercept K_f in the graph. K_f is the Freundlich constant, and n is the exponent of the Freundlich number.

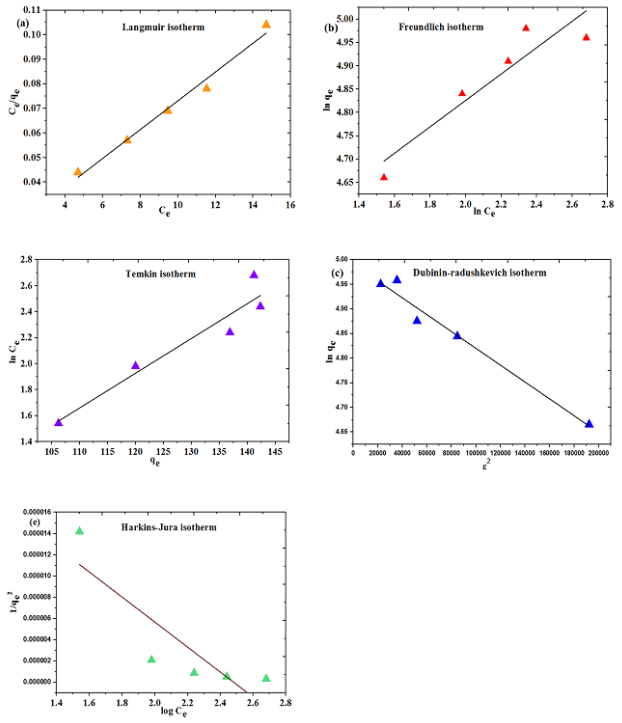

Figure 7. (a) - Langmuir isotherm plot; (b) Freundlich isotherm plot; (c) Temkin isotherm plot; (d) Dubinin Radushkevich isotherm; (e) Harkins - Jura isotherm plot for the removal of sunset yellow dye.

Equation 5 represents the Temkin isotherm model in its non-linear form.

$$\frac{X}{m} = B\ln A + B\ln C_e \quad (5)$$

Where, B_T denotes the Temkin isotherm constant related to the heat of biosorption (KJ/mol). A_T represent Temkin isotherm equilibrium binding constant (L/g).

Dubinin-radushkevich isotherm model is given by Equation.6

$$\ln q_e = \ln q_D - B_D(\varepsilon)^2 \quad (6)$$

where ε represents the mean free energy of adsorption (kJ/mol) can be determined by using Equation 7

$$\varepsilon = RT\ln\left(1+\frac{1}{C_e}\right) \quad (7)$$

Harkins -Jura isotherm investigates the multilayer adsorption model and it accounts for the heterogenous pore distribution phenomenon. It is represented in Equation 8

$$\frac{1}{q_e^2} = \frac{B}{A} - \frac{1}{A\log C_e} \quad (8)$$

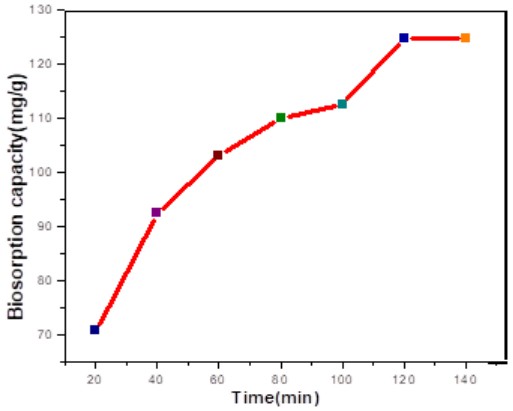

Figure 8. Effect of contact time for the adsorption of sunset yellow dye using MFPW adsorbent.

Figure 7 shows the isotherm plots for SYFCF adsorption onto MFPW and their corresponding kinetic parameters and regression coefficients are presented in Table 2. From Table 2, the higher order of regression coefficient follows: Langmuir > DR > Freundlich > Temkin > HJ isotherm. There was an indication of chemical adsorption if free mean energy (E) was between 8 and 16 kJ/mol. According to the literature, in this study, the free energy value of 0.5kJ/mol is lower than 8 kJ/mol. Hence, it is understood that this might be due to electrostatic or van der Waals interactions, and the adsorption of sunset yellow FCF dye onto MFPW adsorbent was concluded to be a physisorption process. Based on regression coefficients of 0.99, it can be concluded that the Langmuir isothermal model showed the best fit with a maximum adsorption capacity of 200 mg/g for adsorption of sunset yellow FCF dye onto MFPW.

3.5. Effect of contact time and kinetic studies:

Figure 8 shows the effect of contact time for SY FCF dye adsorption onto MFPW. And the experiments were conducted at varying contact with pH 3.0, 50mg/L of initial dye concentration, and a shaking speed of 120 rpm at 30ºC.

It was discovered that the maximum adsorption capacity increases from 20 minutes to 100 minutes, and saturation occurs when the number of vacant sites reaches 100 minutes. During the first 100 minutes, the biosorption capacity increased from 70.8 mg/g to 124.7 mg/g due to the presence of ions that may precipitate the dye molecules.

Table 2. Estimated constants of Langmuir, Freundlich, Temkin, Dubinin–Radushkevich and Harkins-Jura isotherms for adsorption of sunset yellow dye

Isotherm	Parameters	Values
Langmuir	q_m (mg g^{-1})	200
	B(Lmg^{-1})	0.35
	R^2	0.99
Freudlich	K_F	71.88
	N	3.70
	R^2	0.925
Temkin	A (L g^{-1})	6.296
	RT/b_T	32.53
	R^2	0.90
Dubinin–Radushkevich	q_s(mg/g)	5.004
	k_{ad} (mol^2/J^2)	$2x10^{-6}$
	E (kJ/mol)	0.5
	R^2	0.989
Harkins – jura isotherm	A	1×10^5
	B	3×10^{10}
	R^2	0.752

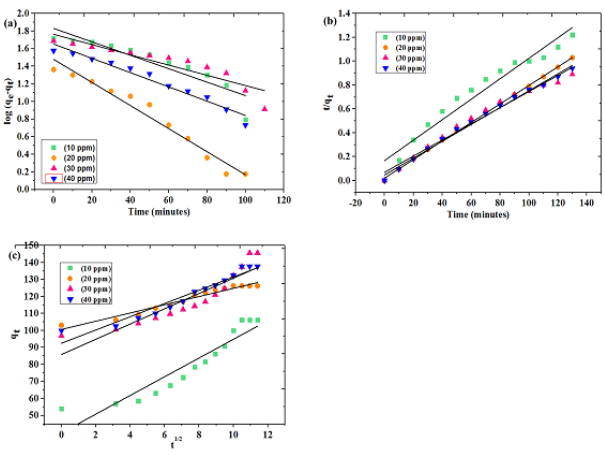

Figure 9. Pseudo first order kinetics (b) Pseudo second order kinetics (c) Intraparticle diffusion for the removal of Sunset yellow dye using MFPW adsorbent.

The kinetic studies are helpful to understand the dynamics controlling mechanism of the adsorption process. The experimental data were analysed using three kinetic models (Figure 9) such as pseudo-first-order, pseudo-second-order, and intraparticle diffusion to investigate the mechanism controlling dye adsorption onto mixed fruit peel waste. [Husseien *et al*., 2007]

3.5.1. Pseudo-first-order model

An assumption in the pseudo-first-order kinetic model was that the rate of adsorbate removal changes with time. Thus, the adsorption capacity of the adsorbent changes. This is the linearized form of the pseudo-first-order kinetic equation.

$$\log(q_e - q_t) = \log q_e - \frac{k_1}{2.303} t \quad (9)$$

Pseudo-first-order model constant k_1 represents the adsorption capacity (mg/g) at equilibrium time and the adsorption capacity (mg/g) at any point in time. [Husseien *et al*., 2007]

3.5.2. Pseudo-second-order model

Electron-sharing between dye and adsorbent functional groups forms the basis of this model, which assumes that adsorption occurs after chemisorption. The following is the formula:

$$\frac{t}{q_t} = \frac{1}{k_2 q_e^2} + \frac{t}{q_e} \quad (10)$$

Where k_2 indicate the rate constant of the pseudo-second-order kinetic model(g/mg min).

When determining k_2, linear plots were drawn, and values of k_2 and q_e can be estimated from the slope and intercept of the respective plot. [Husseien *et al*., 2007]

3.5.3. Intraparticle diffusion model

The adsorption capacity changes with the square root of time in an intraparticle diffusion model, as shown in the following equation.

$$q_t = k_{id} t^{0.5} + C_i \quad (11)$$

Where k_3 denotes the constant of intraparticle diffusion model and C indicate boundary layer thickness (mg/g). This model helps to analyse the diffusion among the adsorbate and adsorption. [Machrouhi *et al*., 2017]

Table 3 lists the kinetic constants and R^2 values that were estimated. An R^2 value greater than 0.9 for pseudo-second-order kinetics that can be seen from the table. Predicted q_e from pseudo-second-order kinetics was in close agreement with the q_e measured. Electrostatic interactions were solely

responsible for sunset yellow dye being adsorbed by fruit peel biosorbents, according to pseudo-second-order adsorption kinetics.

Table 3. Estimated kinetic constants for adsorption of sunset yellow dye using MFPW biosorbent

Kinetics	Parameters	10 ppm	20ppm	30ppm	40ppm
Pseudo first order kinetics	Q_e(mg/g)	5.82	4.63	5.70	5.40
	K_1(min^{-1})	0.016	0.029	0.009	0.018
	R^2	0.83	0.97	0.88	0.96
Pseudo second order kinetics	Q_e(mg/g)	125	142.85	166.67	142.85
	K_2(min^{-1})	0.003	0.0024	0.00052	0.0010
	R^2	0.95	0.999	0.977	0.993
Intraparticle diffusion model	K_3(mg/g $min^{1/2}$)	5.5	2.416	4.489	3.896
	C (mg/g)	39.81	100.6	85.87	92.50
	R^2	0.88	0.961	0.845	0.942

Table 4. Thermodynamic parameters for ST FCF adsorption using MFPW adsorbent

C_o(mg/L)	T(K)	ΔG°(KJ/mol)	ΔH°(KJ/mol)	ΔS°(KJ/mol)	R^2
10	303	-24.347	24.617	0.163	0.95
	313	-26.621			
	323	-28.258			
20	303	-23.725	24.755	0.16	0.99
	313	-25.325			
	323	-26.925			
30	303	-21.117	25.848	0.155	0.90
	313	-22.667			
	323	-24.217			
40	303	-18.751	41.849	0.2	0.99
	313	-20.751			
	323	-22.751			

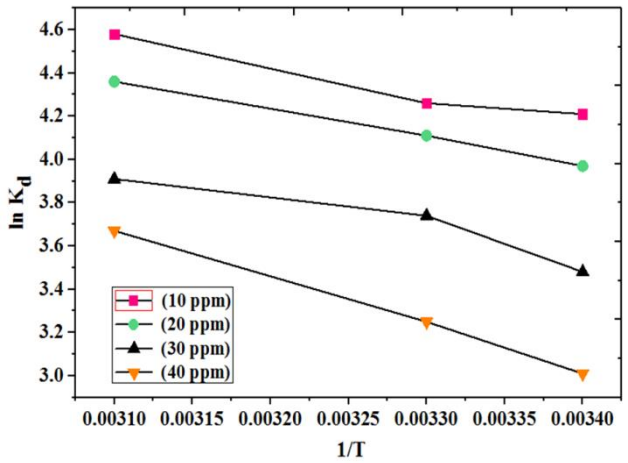

Figure 10. Thermodynamic studies for the removal of Sunset yellow dye using FPW adsorbent.

3.6. Effect of temperature on dye adsorption

Sunset yellow dye adsorption was studied in the 30-50°C range, with an adsorbent dose of 2.0 g/100 ml, pH 3.0, and two hours of contact time. Figure 10 represents the thermodynamics studies on SY FCF adsorption onto MFPW for various concentrations at different temperatures. And a summary of respective thermodynamic parameters ΔGº, ΔHº, and ΔSº are presented in Table 4. The Gibbs free energies (ΔGº) were found to be negative, indicating the adsorption of sunset yellow dye onto MFPW adsorbent to be both spontaneous and feasible, which does not require an external source for the process Adsorption of the sunset yellow dye produced positive enthalpy change (ΔHº) values at various concentrations. Results were endothermic because the activation of dye molecules at the aligned sites of the fruit peels occurred as a result of an increase in temperature. Adsorption sites in MFPW adsorbent that are empty become more and more attractive to anions with increasing temperature. The positive values of entropy change (ΔSº) indicated less randomness in their structural arrangement. [Olu-Owolabi *et al*., 2010].

3.7. Comparison of different adsorbents with mixed fruit peel adsorbent for the removal of sunset yellow

The maximum adsorption capacity for removing SY FCF dye using MFPW was compared with other such adsorbents. And Table 5 summarises the comparision of maximum adsorption capacities for the removal of sunset yellow FCF dye using various fruit peel waste. Mixed Fruit peel waste adsorbent has a higher adsorption capacity (200 mg/g) for sunset yellow FCF dye uptake than the other adsorbents, which provides the surface area sites with well-developed pores for the adsorption of dye.

3.8. Cost evaluation and feasibility of MFPW

The preparation cost of any adsorbent is one of the most subtle characters to understand the economic feasibility of the industrial wastewater treatment. Hence, low-cost adsorbents with enhanced adsorptive properties are

comparable to the available commercial adsorbents [Jayalakshmi and Jeyanthi, 2022]. The raw materials here were collected as waste from the fruit shop, which is discarded as garbage. Those wastes were collected at nil cost and hence required energy cost for the transportation charge and power consumption of chopping, shredding, drying and grinding of raw materials. Therefore, it was estimated to be 200INR/kg, and it was cost-effective compared to other adsorbents.

Table 5. Comparison of maximum adsorption capacity of sunset yellow dye using fruit peel biosorbent with previous studies

Adsorbent	Adsorbate	Qmax (mg/g)	Reference
Treated fruit waste	Rhodamine B and methylene blue	34.48 35.71	Parimaladevi *et al.*, 2011
Pomegranate peel activated carbon	Remazol brilliant blue reactive dye	370.86	Ahmad *et al.*, 2014
Green Pea Peels (Pisum sativum)	Methylene blue	163.94	Dod *et al.*, 2012
Coconut (Cocos nucifera) bunch waste	Methylene blue	70.92	Hameed *et al.*, 2008
Papaya seeds	Methylene blue	555.557	Hameed, 2009
Orange peel carbon	Direct yellow 12	75.76	Khaled *et al.*, 2009
Alligator weed activated carbon	Sunset yellow	271	Kong *et al.*, 2017
Cadmium Sulfide Nanoparticle Loaded on Activated Carbon	Sunset yellow	83.3	Mosallanejad *et al.*, 2017
Carica papaya wood	Methylene blue	63.29	Nguyen *et al.*, 2020
Leaf residues of Thymus numidicus (RTN), Origanum glandulosum (ROG) and Sapindus mukorossi pericarp fibre (SMPF)	Methylene blue	24.2, 33.3 and 41	Djamila Youcef *et al.*, 2021
Positively charged biochar	Sunset yellow	74.07	Mahmoud *et al.*, 2020
Zinc oxide nanorods loaded on activated carbon	Sunset yellow	142.85	Maghsoudi *et al.*, 2015
Activated carbon derived from cassava sievate biomass	Sunset yellow	0.091	Chukwuemeka *et al.*, 2021
Steam-activated carbon from malt bagasse	Sunset yellow	199.7	Lopes *et al.*, 2021
Copper doped ZnS nanoparticles loaded on activated carbon	Sunset yellow	85.397	Agarwal *et al.*, 2016
Mixed fruit peel waste	Sunset yellow	200	Present study

The preparation of MFPW is simple since neither special equipment nor expertise handling is required. Also, it is biocompatible, sustainable and environmentally friendly since it is biomass waste. Furthermore, it is cost-effective and easy to scale up. These results altogether make the Mixed fruit peel waste a promising candidate for removing dye from an aqueous solution.

4. Conclusion

A biosorbent made from prepared mixed fruit peel waste was used to remove the sunset yellow FCF dye successfully. According to the batch studies, the maximum adsorption capacity was 200 mg/g at pH 3.0, contact time of 100 minutes, adsorbent dose of 2.0g, and initial dye concentration of 40ppm. The regression coefficient for Langmuir isotherm data was more significant than or equal to 0.9, making it the best fit. The best adsorption kinetics are described by pseudo-second-order kinetics. The adsorption capacity of the mixed fruit peel waste adsorbent was higher than other such adsorbents. This study discovered that the highly exposed adsorption sites facilitate the adsorption mechanism. Therefore, it can be used as a cost-effective, eco-friendly ansd sustainable biosorbent for the efficient removal of textile dyes.

Acknowledgments

The first author wishes to thank the Principal and Head of Industtrial Biotechnology Department, Government College of Technology, Coimbatore, for providing facilities to carry out the current study.

References

Agarwal S., Tyagi I., Gupta V.K., Dastkhoon M., Ghaedi M., Yousefi F., and Asfaram A. (2016). Ultrasound-assisted adsorption of Sunset Yellow CFC dye onto Cu doped ZnS nanoparticles loaded on activated carbon using response surface methodology based on central composite design. *Journal of Molecular Liquids*, **219**, 332–340.

Ahmad M.A., Eusoff M.A., Adegoke K.A., and Bello O.S. (2021). Sequestration of methylene blue dye from aqueous solution using microwave assisted dragon fruit peel as adsorbent. *Environmental Technology & Innovation*, ***24***, 101917.

Ahmad M.A., Puad N.S.A., and Bello O.S. (2014). Kinetic, equilibrium and thermodynamic studies of synthetic dye removal using pomegranate peel activated carbon prepared

by microwave-induced KOH activation. *Water Resources and Industry,* **6**, 18–35. https://doi.org/10.1016/j.wri.2014.06.002.

Aksu Z. and Balibek E. (2010). Effect of salinity on metal-complex dye biosorption by Rhizopus arrhizus. *Journal of environmental management,* **91**(7), 1546–1555. https://doi.org/10.1016/j.jenvman.2010.02.026.

Almeida-Naranjo C.E., Aldás M.B., Cabrera G., & Guerrero V.H. (2021). Caffeine removal from synthetic wastewater using magnetic fruit peel composites: Material characterization, isotherm and kinetic studies. *Environmental Challenges*, **5**, 100343.

Auta M. and Hameed B.H. (2011). Optimized waste tea activated carbon for adsorption of Methylene Blue and Acid Blue 29 dyes using response surface methodology. *Chemical Engineering Journal*, **175**: 233–243. https://doi.org/10.1016/j.cej.2011.09.100.

Barka N., Assabbane A., Nounah A., Laanab L., and Ichou Y.A. (2009). Removal of textile dyes from aqueous solutions by natural phosphate as a new adsorbent, *Desalination* **235**(1-3), 264–275. https://doi.org/10.1016/j.desal.2008.01.015.

Bhatnagar A. and Minocha A.K. (2009). Adsorptive removal of 2, 4-dichlorophenol from water utilizing Punica granatum peel waste and stabilization with cement. *Journal of hazardous materials,* **168**(2–3), 1111–1117. https://doi.org/10.1016/j.jhazmat.2009.02.151.

Chukwuemeka-Okorie H.O., Ekuma F.K., Akpomie K.G., et al. (2021). Adsorption of tartrazine and sunset yellow anionic dyes onto activated carbon derived from cassava sievate biomass. *Applied Water Science*, **11**, 27. https://doi.org/10.1007/s13201-021-01357-w.

Dod R., Banerjee G., and Saini S. (2012). "Adsorption of methylene blue using green pea peels (Pisum sativum): A cost-effective option for dye-based wastewater treatment." *Biotechnology and Bioprocess Engineering,* **17**(4), 862–874. https://doi.org/10.1007/s12257-011-0614-5.

Gao H., Wang Y., and Zheng L. (2013). Hydroxyl-functionalized ionic liquid-based cross-linked polymer as highly efficient adsorbent for anionic azo dyes removal. *Chemical Engineering Journal*, **234**, 372–379. https://doi.org/10.1016/j.cej.2013.08.078

Garba Z.N., Zhou W., Zhang M., and Yuan Z. (2019). A review on the preparation, characterization and potential application of perovskites as adsorbents for wastewater treatment. *Chemosphere*, doi: https://doi.org/10.1016/j.chemosphere.2019.125474.

Garg V.K., Gupta R., Yadav A.B., and Kumar R. (2003). Dye removal from aqueous solution by adsorption on treated sawdust. *Bioresource and Technology,* **89**, 121–124. https://doi.org/10.1016/S0960-8524(03)00058-0.

Georgin J., da Boit Martinello K., Franco D.S., Netto M.S., Piccilli D.G., Yilmaz M., Silva L.F.O., and Dotto G.L. (2021). Residual Peel of Pitaya Fruit (Hylocereus undatus) as a Precursor to Obtaining an Efficient Carbon-based Adsorbent for the Removal of Metanil Yellow Dye From Water. *Journal of Environmental Chemical Engineering*, 107006.

Gupta S.A., Vishesh Y., Sarvshrestha N., Bhardwaj A.S., Kumar P.A., Topare N.S., Raut-Jadhav S., Bokil S.A., and Khan A. (2021). "Adsorption isotherm studies of Methylene blue using activated carbon of waste fruit peel as an adsorbent. *Materials Today: Proceedings* .

Hameed B.H. (2009). "Evaluation of papaya seeds as a novel non-conventional low-cost adsorbent for removal of methylene blue. *Journal of Hazardous Materials*, **162**(2–3), 939–944. https://doi.org/10.1016/j.jhazmat.2008.05.120.

Hameed B.H., Mahmoud D.K., and Ahmad A.L. (2008). Equilibrium modeling and kinetic studies on the adsorption of basic dye by a low-cost adsorbent: Coconut (Cocos nucifera) bunch waste." *Journal of Hazardous Materials*, **158**(1), 65–72. https://doi.org/10.1016/j.jhazmat.2008.01.034

Hossain N., Bhuiyan M.A., Pramanik B.K., Nizamuddin S., and Griffin G. (2020). Waste materials for wastewater treatment and waste adsorbents for biofuel and cement supplement applications: a critical review. *Journal of Cleaner Production*, **255**, 120261. https://doi.org/10.1016/j.jclepro.2020.120261

Hussain S., Ullah Z., Gul S., Khattak R., Kazmi N., Rehman F., Khan S., Ahmad K., Imad M., and Khan A. (2016). Adsorption characteristics of magnesium-modified bentonite clay with respect to acid blue 129 in aqueous media. *Polish Journal of Environmental Studies,* **25**(5), 1947–1953. https://doi.org/10.15244/pjoes/62272

Husseien M., Amer A.A., El-Maghraby A., and Taha N.A. (2007). Utilization of barley straw as a source of a activated carbon for removal of methylene blue from aqueous solution. *Journal of Applied Sciences Research,* **3**(11), 1352–1358.

Idris M.N., Ahmad Z.A., Ahmad M.A., Ahmad N., and Sulaiman S.K. (2011). Optimization of process variables for malachite green dye removal using rubber seed coat based activated carbon. *International Journal of Engineering & Technology*, **11**(1), 234–240.

Jayalakshmi R., & Jeyanthi J. (2021). Dynamic modelling of Alginate-Cobalt ferrite nanocomposite for removal of binary dyes from textile effluent. *Journal of Environmental Chemical Engineering*, **9**(1), 104924. https://doi.org/10.1016/j.jece.2020.104924

Jayalakshmi R., Jeyanthi J., & Sidhaarth K.A. (2022). Versatile Application of Cobalt Ferrite Nanoparticles for the Removal of Heavy Metals and Dyes from Aqueous Solution. *Environmental, Nanotechnology, Monitoring & Management*, **17**, 100659.

Jiang Z., Xie J., Jiang D., Yan Z., Jing J., Liu D. (2014). Enhanced adsorption of hydroxyl contained/anionic dyes on non functionalized Ni@SiO2 core–shell nanoparticles: Kinetic and thermodynamic profile. *Applied Surface Science*, **292**(15),301–310. https://doi.org/10.1016/j.apsusc.2013.11.136

Khaled A., Nemr A.E., El-Sikaily A., and Abdelwahab O. (2009). Treatment of artificial textile dye effluent containing Direct Yellow 12 by orange peel carbon. *Desalination,* **238**(1–3), 210–232. https://doi.org/10.1016/j.desal.2008.02.014

Khaskheli M.I., Chandio Z.A., Khan S., Khokhar F.M., Memon A.G., Jatoi W.B., Khokhar L.A.K., and Shahani N.K. (2021). The utilization of okra leaves as an agricultural waste for the removal of As(III) and As(V). *Global NEST Journal*, **23**(2), 257–264.

Kong, Q., Qun L., Miao M.S., Liu Y.Z., Chen Q.F., and Zhao C.S. (2017). Kinetic and equilibrium studies of the biosorption of sunset yellow dye by alligator weed activated carbon. *Desalination and Water Treatment,* **66**, 281–290.

Lim L.B., Priyantha N., Latip S.A.A., Lu Y.C., & Mahadi A.H. (2020). Converting Hylocereus undatus (white dragon fruit) peel waste into a useful potential adsorbent for the removal of toxic Congo red dye. *Desalination Water Treat*, **185**, 307–317. doi: 10.5004/dwt.2020.25390

Liu X., Tiana J., Li Y., Suna N., Mia S., Xiea Y., Chen Z. (2019). Enhanced dyes adsorption from wastewater via Fe_3O_4 nanoparticles functionalized activated carbon. *Journal of Hazardous Materials*, **373**(5), 397–407. https://doi.org/10.1016/j.jhazmat.2019.03.103.

Liu Y., Ohko Y., Zhang R., Yang Y., and Zhang Z. (2010). Degradation of malachite green on Pd/WO_3 photocatalysts under simulated solar light. *Journal of Hazardous Materials,* **184**, 386–391. https://doi.org/10.1016/j.jhazmat.2010.08.047.

Lopes G.K., Zanella H.G., Spessato L., Ronix A., Viero P., Fonseca J.M., and Almeida V.C. (2021). Steam-activated carbon from malt bagasse: Optimization of preparation conditions and adsorption studies of sunset yellow food dye. *Arabian Journal of Chemistry*, **14**(3), 103001.

Machrouhi A., Farnane M., Elhalil A., Elmoubarki R., Abdennouri M., Qourzal S., Tounsadi H., and Barka N. (2017). Effectiveness of beetroot seeds and H3PO4 activated beetroot seeds for the removal of dyes from aqueous solutions. *Journal of Water Reuse and Desalination*. doi: 10.2166/wrd.2017.034

Mahmoud M.E., Abdelfattah A.M., Tharwat R.M., & Nabil G.M. (2020). Adsorption of negatively charged food tartrazine and sunset yellow dyes onto positively charged triethylenetetramine biochar: Optimization, kinetics and thermodynamic study. *Journal of Molecular Liquids*, **318**, 114297.

Mall I.D., Srivastava V.C., and Agarwal N.K. (2006). "Removal of Orange-G and Methyl Violet dyes by adsorption onto bagasse fly ash—kinetic study and equilibrium isotherm analyses." *Dyes and pigments,* **69**(3), 210–223. https://doi.org/10.1016/j.dyepig.2005.03.013.

Mosallanejad N., and Arami A. (2012). Kinetics and isotherm of sunset yellow dye adsorption on cadmium sulfide nanoparticle loaded on activated carbon. 31–40.

Nguyen T.N.N., Huynh T.T.H., and To T.H. (2020). "Removal of methylene blue from simulated wastewater by Carica papaya wood biosorbent. "*Vietnam Journal of Science, Technology and Engineering* **62**(4), 8–17. https://vietnamscience.vjst.vn/index.php/VJSTE/article/view/366/251.

Olu-Owolabi B.I., and Unuabonah E.I. (2010). Kinetic and thermodynamics of the removal of Zn^{2+} and Cu^{2+} from aqueous solution by sulphate and phosphate-modified Bentonite clay. *Journal of Hazardous Materials,* **184**(1–3), 731–738. https://doi.org/10.1016/j.jhazmat.2010.08.100.

Parimaladevi P., and Venkateswaran V. (2011). Adsorption of cationic dyes (rhodamine B and methylene blue) from aqueous solution using treated fruit waste. *Journal Applied Technology and Environmental Sanitation*,**1** 285–293.

Ramalingam R.J., Sivachidambaram M., Vijaya J.J., Al-Lohedan H.A., amd Muthumareeswaran, M.R. (2020). Synthesis of porous activated carbon powder formation from fruit peel and cow dung waste for modified electrode fabrication and application. *Biomass and Bioenergy*, **142**, 105800.

Rangabhashiyam S., Lata S., and Balasubramanian P. (2017). Biosorption characteristics of methylene blue and malachite green from simulated wastewater onto Carica papaya wood biosorbent. *Surfaces and Interfaces.* https://doi.org/10.1016/j.surfin.2017.09.011.

Ranjithkumar V., Sangeetha S., and Vairam S. (2014). Synthesis of magnetic activated carbon/α-Fe2O3 nanocomposite and its application in the removal of acid yellow 17 dye from water. *Journal of Hazardous Materials* ,**273** 127–135. https://doi.org/10.1016/j.jhazmat.2014.03.034.

Rebitanim N.Z., Ghani W.A.W.A.K., Mahmoud D.K., Rebitanim N.A., and Salleh M.A.M. (2012). Adsorption capacity of raw empty fruit bunch biomass onto methylene blue dye in aqueous solution. *Journal of Purity, Utility Reaction and Environment*, **1**(1), 45–60.

Sahu S., Pahi S., Sahu J.K., Sahu U.K., and Patel R.K. (2020). Kendu (Diospyros melanoxylon Roxb) fruit peel activated carbon—an efficient bioadsorbent for methylene blue dye: equilibrium, kinetic, and thermodynamic study. *Environmental Science and Pollution Research*, **27**(18), 22579–22592. https://doi.org/10.1007/s11356-020-08561-2.

Shoukat S., Bhatti H.N., Iqbal M., and Noreen S. (2017). "Mango stone biocomposite preparation and application for crystal violet adsorption: a mechanistic study." *Microporous and Mesoporous Materials,* **239,** 180–189. https://doi.org/10.1016/j.micromeso.2016.10.004.

Solangi N.H., Kumar J., Mazari S.A., Ahmed S., Fatima N., and Mujawar N.M. (2021). Development of fruit waste derived bio-adsorbents for wastewater treatment: a review. *Journal of Hazardous Materials*, 125848.

Sun Y., and Webley P.A. (2010). Preparation of activated carbons from corncob with large specific surface area by a variety of chemical activators and their application in gas storage. *Chemical Engineering Journal,* **162**, 3, 883–892. https://doi.org/10.1016/j.cej.2010.06.031.

Wong S., Ngadi N., Inuwa I.M., and Hassan O. (2018). Recent advances in applications of activated carbon from biowaste for wastewater treatment: a short review. *Journal of Cleaner Production*, **175**, 361–375.

Youcef D., Fernane F., Hadj-ziane A., and Messara Y. (2021). The kinetics and equilibrium sorption of methylene blue on plant residues in aqueous solution. *Euro-Mediterranean Journal for Environmental Integration,* **6**, 59 https://doi.org/10.1007/s41207-021-00269-0.

Zhiyong Y., Wenhua W., Lin S., Liqin L., Zhiyin W., Xuanfeng J., Chaonan D., Ruiying Q. (2013). Acceleration comparison between Fe^{2+}/H_2O_2 and CO^{2+}/oxone for decolouration of azo dyes in homogeneous systems. *Chemical Engineering Journal*, **234** 475–483. DOI: 10.1016/j.cej.2013.08.013.